

Characterization of microcrystalline silicon thin film solar cells prepared by high working pressure plasma-enhanced chemical vapor deposition

Sung-Do Lee · Young-Joo Lee · Kee-Seok Nam · Yongsoo Jeong ·
Dong-Ho Kim · Chang-Su Kim · Sung-Gyu Park · Se-Hun Kwon ·
Jung-Dae Kwon · Jin-Seong Park

Received: 6 March 2014 / Accepted: 9 May 2014 / Published online: 30 September 2014
© Springer Science+Business Media New York 2014

Abstract Using the high working pressure plasma-enhanced chemical vapor deposition (HWP-PECVD) technique, the hydrogenated microcrystalline silicon ($\mu\text{c-Si:H}$) films for photovoltaic layers of thin film solar cells was investigated. The $\mu\text{c-Si:H}$ films were deposited on surface textured fluorine-doped tin oxide (FTO) glass substrates at 100 Torr in a 100 MHz very high frequency (VHF) plasma of gas mixtures containing He, H_2 , and SiH_4 . It was found that an optimum ratio of the H_2/SiH_4 flow-rate existed for growing a homogenous microcrystalline through the whole film without amorphous incubation layer. When an intrinsic $\mu\text{c-Si:H}$ thin film was deposited at n-i-p single junction solar cell, the cell performances were dependent on with or without an amorphous incubation layer. With an amorphous incubation layer, the open circuit voltage (V_{oc}) of cell was 0.8 V, which was typical cell property of hydrogenated amorphous silicon (a-Si:H). On the other hand, at the optimum ratio of the H_2/SiH_4 flow-rate, $\mu\text{c-Si:H}$ single cell responding an infrared light showed the V_{oc} of 0.4 V.

Keywords Silicon · Microcrystalline · High working pressure · Chemical vapor deposition

1 Introduction

The thin-film silicon solar cell has been attracting considerable attention as high conversion efficiency could be achieved at relatively low manufacturing costs [1]. Hydrogenated microcrystalline silicon ($\mu\text{c-Si:H}$) cell responds mainly from red to infrared light, and the optical absorption coefficients of $\mu\text{c-Si:H}$ at long wavelengths are almost identical to those of the Si single crystal [2]. Because absorption coefficient of $\mu\text{c-Si:H}$ is relatively low, a thickness of 1–2 μm is usually required for $\mu\text{c-Si:H}$ photovoltaic-active layer. Therefore, for achieving a short production time, or for industrializing the solar cell, researches about plasma-enhanced chemical vapor deposition (PECVD) process using very high frequency (VHF, 50–150 MHz) at high pressure (10–750 Torr) have been reported [3–5]. Meanwhile, control of the crystalline volume is crucial because the Si crystallinity has a significant influence on the optical gap, defect density, and conductivity of the materials [6]. The commonest method for controlling the crystalline volume fraction (X_c) of $\mu\text{c-Si}$ is to adjust the dilution ratio of silane (SiH_4) and hydrogen (H_2) gases, or the plasma power.

Here, we fabricated the single junction $\mu\text{c-Si:H}$ thin film solar cells by using a high working pressure plasma-enhanced chemical vapor deposition (HWP-PECVD) system at 100 Torr with a cylindrical rotary electrode; this system is superior to conventional PECVD because it has the following features: a high deposition rate as a result of the high partial pressure of the reactive gas and a high plasma density by the very high frequency of 100 MHz; the ability to control the film uniformity because of the homogeneous distribution of reactants by the rotary electrode system; and low bombardment damage

S.-D. Lee · Y.-J. Lee · K.-S. Nam · Y. Jeong · D.-H. Kim ·
C.-S. Kim · S.-G. Park · J.-D. Kwon (✉)
Surface Technology Division, Korea Institute of Materials Science,
Changwon, Gyeongnam 641-831, Republic of Korea
e-mail: jdkwon@kims.re.kr

S.-H. Kwon (✉)
School of Materials Science and Engineering, Pusan National
University, Busan 609-735, Republic of Korea
e-mail: sehun@pusan.ac.kr

J.-S. Park (✉)
Department of Materials Science and Engineering, Hanyang
University, Seoul 133-719, Republic of Korea
e-mail: jsparklime@hanyang.ac.kr

S.-D. Lee
Department of Applied Hybrid Materials, Graduate School of
Convergence Science, Pusan National University, Busan 609-735,
Republic of Korea

because of the lower kinetic energy [7, 8]. When an intrinsic $\mu\text{-Si:H}$ thin film was deposited at n-i-p single junction solar cell, the cell performances were dependent on with or without an amorphous incubation layer. With an amorphous incubation layer, the cell did not respond an infrared light. On the other hand, when an intrinsic Si film was homogeneous microcrystalline through the whole film, the cell responded an infrared light, and its performance was a behavior of $\mu\text{-Si:H}$ thin film solar cell.

2 Experimental

The HWP-PECVD system used to produce $\mu\text{-Si:H}$ was based on previously reported designs (see Fig. 1) [7, 8]. The diameter of the cylindrical rotary electrode was 300 mm and the width was 240 mm. The HWP-PECVD of $\mu\text{-Si:H}$ was performed on 1.8-mm-thick soda-lime glass (200×200 mm) substrates at 200°C , with a deposition pressure of 100 Torr. Before deposition, the base pressure of the chamber was reduced to 2×10^{-6} Torr, using dry and turbo molecular pumps. After closing the main valve connected to the turbo molecular pump, helium (He), H_2 , and SiH_4 gases were simultaneously injected into the chamber until a pressure of 100 Torr was attained, and continuously supplied into the reaction chamber during Si film deposition. The purity of the gases was 99.999%. The $\text{SiH}_4 + \text{H}_2$ concentration was 4% and the ratios of the H_2/SiH_4 flow-rates was 13–35. The electrode rotation speed was 1,000 rpm, and the deposition gap between the electrode and the substrate was 0.5 mm. The substrate scan distance was 150 mm and the scan speed was fixed at 10 mm/s. An impedance matching unit supplied 100 MHz VHF power of 20 W/cm^2 to the electrode.

The Si film thickness on surface textured fluorine-doped tin oxide (FTO) glass [NSG TECTM 8 of PILKINGTON] was measured by α -step (TENCOR P-11). For confirmation of the Si crystalline volume fraction, Raman spectra were measured using a Jobin Yvon LabRam HR800 (Horibo, Ltd., Kyoto,

Japan) UV/micro-Raman spectrometer at room temperature. The measurements were carried out at 632.8 nm using a HeNe laser, below 50 mW to avoid thermally induced crystallization. The microstructures of the films were observed by transmission electron microscopy (TEM: JEM-2100F, JEOL, Tokyo, Japan) at 200 kV. The TEM specimens for cross-sectional observations were prepared by using Ar ion source of 3.2 keV with precision ion polishing system (PIPS). Secondary ion mass spectrometry (SIMS) depth profiles were performed to determine the concentration of oxygen and nitrogen in the $\mu\text{-Si:H}$ layer using magnetic sector instrument (CAMECA, model: IMS 7f). Primary Cs^+ ions at near-normal incidence with energies of 6 keV were used and negative secondary ions were detected.

For the process of manufacturing the solar cells, the cell structure was glass substrate/textured FTO/aluminum-doped zinc oxide (AZO)/p-i-n/metal electrode. The 100 nm thick AZO film was deposited by sputter system to protect FTO from hydrogen plasma. Only the i-layer with thickness of 1 μm was deposited by HWP-PECVD, and the p- and n-layers with thickness of about 30 nm were formed by conventional low-pressure PECVD. Thus, the p/i and i/n interfaces of those cells were exposed to the air during the specimen transfer. For the metal electrode, silver was thermally deposited in a high vacuum chamber ($\sim 2 \times 10^{-6}$ Torr) using a shadow mask to define a cell active area of 0.25 cm^2 . The FTO glass contained nine cells and the cell performance was considered to be the average value determined after measuring the performances of nine cells. Current density-voltage (J - V) characteristics were measured using a Keithley 2,400 source meter under 100 mW/cm^2 (AM 1.5G) irradiation from a solar simulator (Pecell Technologies Inc., PEC-L11). In addition to the photovoltaic performance, external quantum efficiency (EQE) of each photovoltaic device was obtained by using a 200 W Xe lamp and a grating monochromator, and the light intensity was measured by a calibrated Si solar cell (PV measurement).

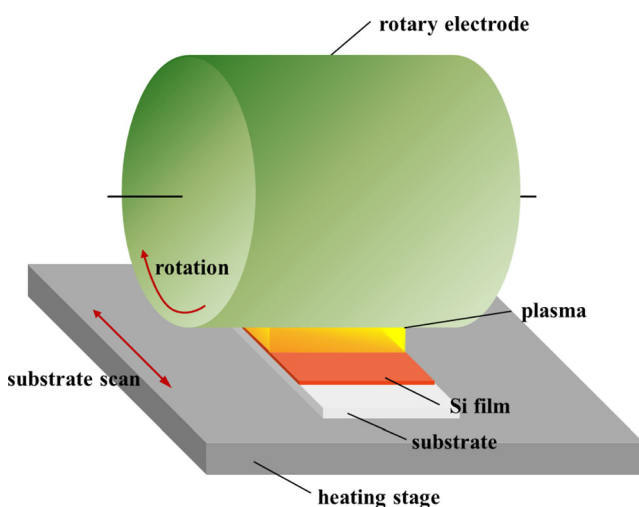
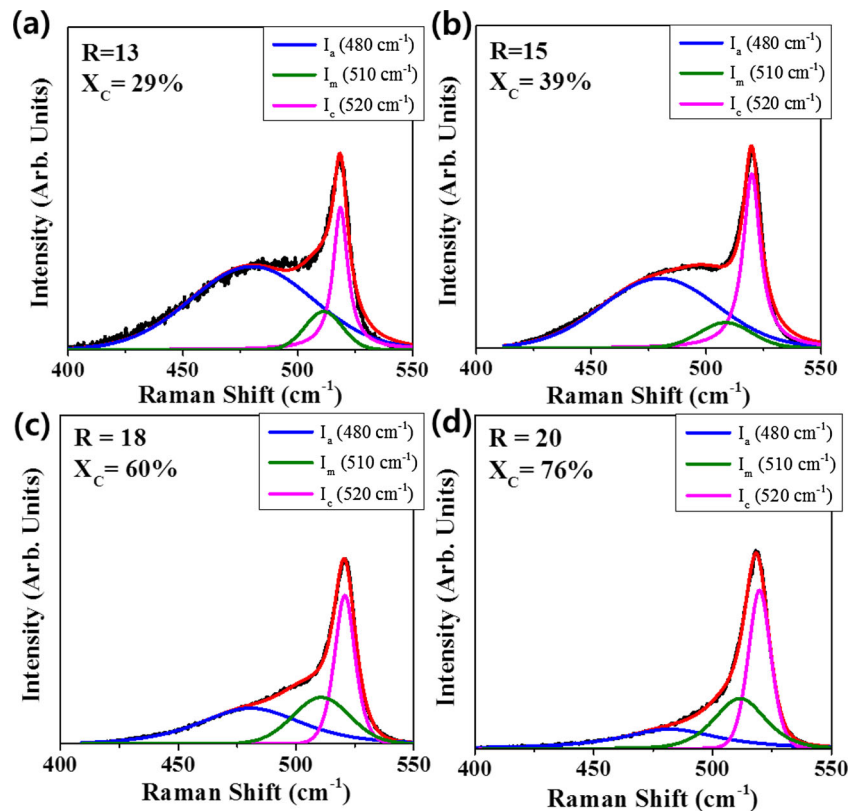


Fig. 1 Schematic illustration of the experimental setup

3 Results and discussion

The crystallinity of the Si films was confirmed by Raman spectroscopy, as shown in Fig. 2. All the about 1 μm thick Si films were deposited on the textured FTO glass substrate because the films peeled off on bare glass substrate owing to the residual stress of $\mu\text{-Si}$. The Si transverse optical (TO) peaks were deconvoluted into their integrated crystalline Gaussian peak (I_c , $\sim 520 \text{ cm}^{-1}$), amorphous Gaussian peak (I_a , $\sim 480 \text{ cm}^{-1}$), and intermediate Gaussian peak (I_m , $\sim 510 \text{ cm}^{-1}$) [9, 10]. Following this, the crystalline volume fraction (X_c) was calculated from the simple equation, $X_c = (I_c + I_m)/(I_c + I_m + I_a)$. The X_c increased from 29 to 76 % when the ratios of H_2/SiH_4 flow-rates (R) increased from 13 to

Fig. 2 Raman spectra of $\mu\text{c-Si:H}$ films grown at the ratio of H_2/SiH_4 flow-rates (R) (a) 13, (b) 15, (c) 18, and (d) 20. The Si crystalline volume fraction of the films increased from 29 to 76 % with the ratios of H_2/SiH_4 flow-rates



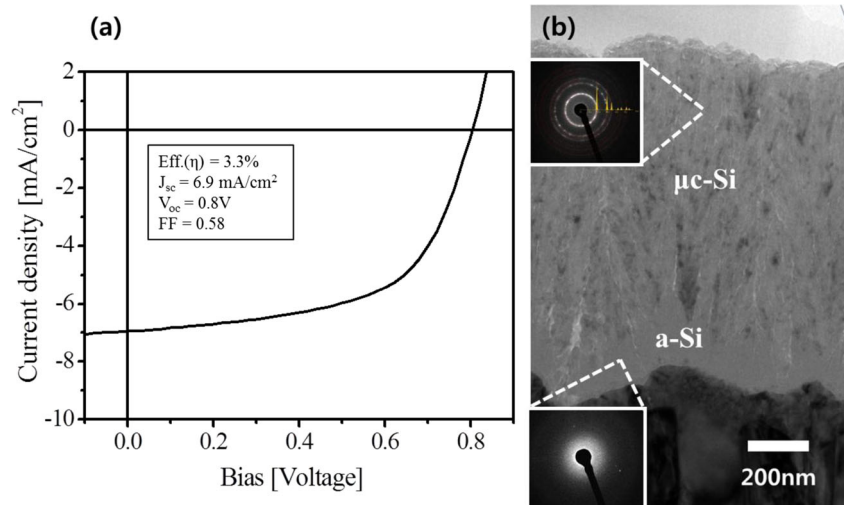
20. It has been widely known that the increase in H_2/SiH_4 flow ratio leads to an increase in the crystalline volume fraction of Si thin films. Basically, two kinds of mechanisms, namely etching by hydrogen atoms and chemical annealing, have been proposed to explain the growth of crystalline Si [11].

In order to fabricate the $\mu\text{c-Si:H}$ n-i-p single junction solar cell, intrinsic $\mu\text{c-Si}$ layer was deposited by HWP-PECVD at $R=18$. The thickness of i-layer was about $1 \mu\text{m}$ by regulating the number of substrate scanning on a large area ($200 \times 200 \text{ mm}$). We measured the cell performances of the J - V characteristic, including short-circuit current (J_{sc}), open-circuit voltage (V_{oc}), and fill factor (FF), as shown in Fig. 3(a). The conversion efficiency of 3.3 % (J_{sc} : 6.9 mA/cm^2 ; V_{oc} : 0.8 V ; and FF: 58 %) has been achieved. Specially, the open circuit voltage (0.8 V) of the cell is higher than that of previous reports (0.5 V) in $\mu\text{c-Si}$ thin film solar cell [3, 12]. The V_{oc} of hydrogenated amorphous silicon (a-Si:H) single cell is usually $0.8 \sim 0.9 \text{ V}$ [13, 14]. T. Matsui et al. reported that V_{oc} of $\mu\text{c-Si}$ single solar cell increased from 0.4 to 0.5 V as the crystalline volume fraction in intrinsic Si layer decreased from 80 to 50 % [15]. However, the X_c of HWP-PECVD $\mu\text{c-Si:H}$ single cell with V_{oc} (0.8 V) was 60 %. To investigate the microstructure of the deposited HWP-PECVD $\mu\text{c-Si}$ thin film, cross-sectional TEM observations was performed as shown in Fig. 3(b). The film exhibited that 800 nm thick microcrystalline Si grew on the initial 200 nm thick amorphous incubation

layer on the textured FTO glass. The inset shows the diffraction patterns of each layer. The diffraction pattern in the $\mu\text{c-Si:H}$ layer indicated peaks corresponding to cubic polycrystalline phase Si in the (111), (220), and (311) lattice planes, however the diffraction pattern for a-Si:H layer exhibited fuzzy rings and was shadowy. According to the growth dynamics of $\mu\text{c-Si:H}$, it nucleates from within the growing a-Si:H phase after a critical phase-transition (amorphous to crystalline) thickness that decreases with increasing H_2 dilution ratio [16]. Thus, it seemed that the high V_{oc} of 0.8 V was generated by intrinsic amorphous incubation layer.

Figure 4 shows the crystallinities of the about 200 nm thick Si films, confirmed by Raman spectroscopy to exclude the effect of amorphous incubation layer. It was revealed that an amorphous Si film was formed when the 200 nm thick intrinsic Si was deposited at $R=20$, as shown in Fig. 4(a). Although the X_c of $1 \mu\text{m}$ thick intrinsic Si layer was 76 %, the 200 nm thick Si exhibited an amorphous phase. The penetration depth of the excitation light used in Raman spectroscopy is less than $0.2 \sim 0.3 \mu\text{m}$; thus the obtained $X_c=76\%$ value should reflect the $\mu\text{c-Si:H}$ just adjacent to the film surface. In the case of 200 nm thick Si films, a peak at around 520 cm^{-1} being attributed to the crystalline Si phase is clearly observed at $R=25$. And the X_c increased from 35 to 69 % as the ratios of H_2/SiH_4 flow-rates (R) increased from 25 to 35. It was confirmed that the high $R=25$ was required to decrease the

Fig. 3 (a) Photocurrent vs voltage characteristic of solar cell with $\mu\text{-Si:H}$ i-layer deposited at the ratio of H_2/SiH_4 flow-rate of 18. (b) Cross-sectional image of the solar cell with $\mu\text{-Si:H}$ i-layer deposited by HWP-PECVD at the ratio of H_2/SiH_4 flow-rates of 18



critical phase-transition (amorphous-to-microcrystalline) thickness.

In order to fabricate the $\mu\text{-Si:H}$ n-i-p single junction solar cell without the amorphous incubation Si layer, we performed the two-step intrinsic Si deposition process in which a 200 nm thick $\mu\text{-Si:H}$ film was deposited at $R=30$, and then the ratio of H_2/SiH_4 flow-rates was changed to 20. The two-step process was to prevent excessive Si grain growth which may induce the increase of defect density and decrease of

photosensitivity [17]. Figure 5(a) shows the two-step intrinsic $\mu\text{-Si:H}$ cell performances of the J - V characteristic. The open circuit voltage was 0.4 V, which was typical cell property of $\mu\text{-Si:H}$ n-i-p single junction solar cell. By injecting a high hydrogen gas at the initial Si film growth, the amorphous incubation layer was not observed through the cross-sectional TEM image, as shown in Fig. 5(b). Figure 5(c) shows the EQE spectra for two $\mu\text{-Si:H}$ single junction solar cells, which were intrinsic Si thin films deposited by $R=18$,

Fig. 4 Raman spectra of $\mu\text{-Si:H}$ films grown at the ratio of H_2/SiH_4 flow-rates (R) (a) 20, (b) 25, (c) 30, and (d) 35. The Si crystalline volume fraction of the films increased from 0 to 69 % with the ratios of H_2/SiH_4 flow-rates

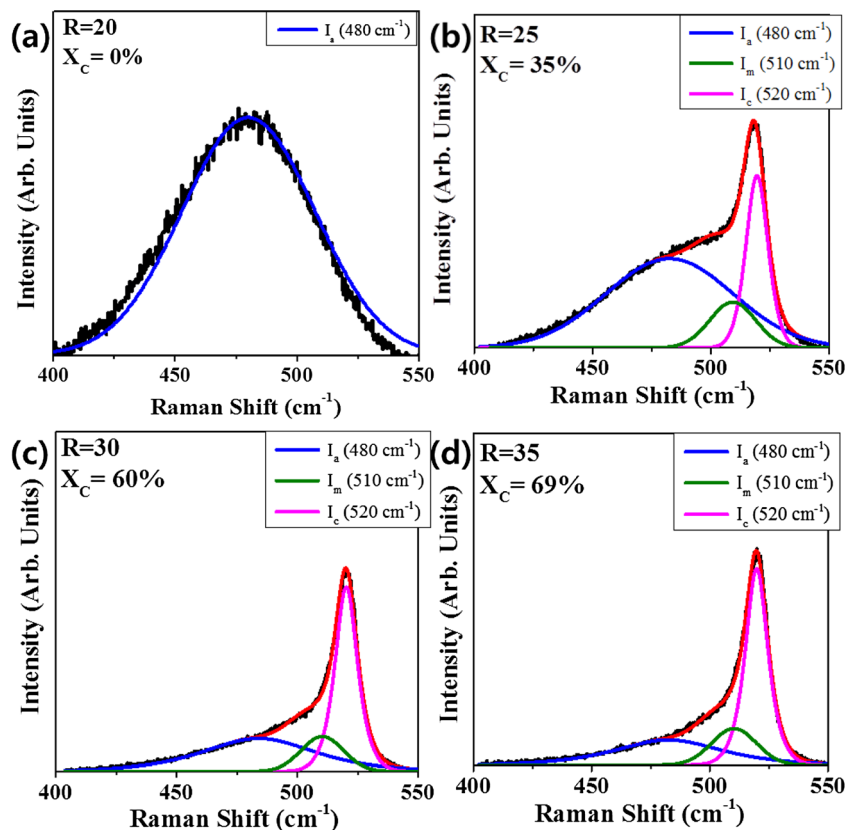
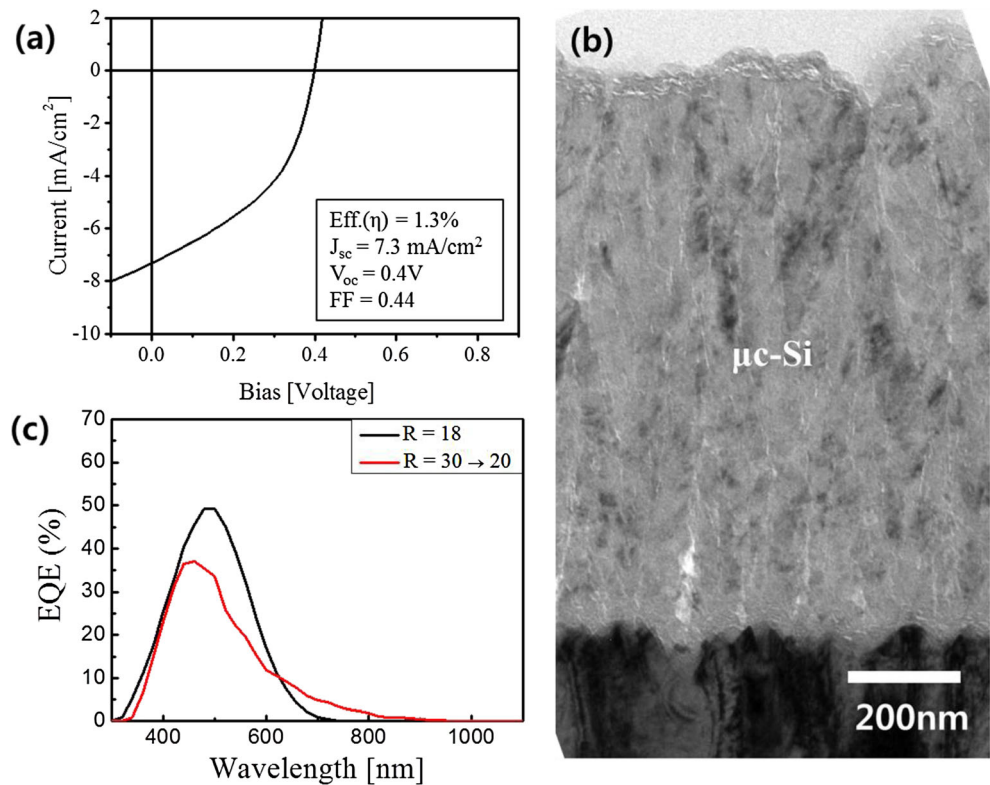


Fig. 5 (a) Photocurrent vs voltage characteristic of solar cell with $\mu\text{-Si:H}$ i-layer deposited by two-step process at the ratios of H_2/SiH_4 flow-rates of 30→20. (b) Cross-sectional image of the solar cell with $\mu\text{-Si:H}$ i-layer deposited by HWP-PECVD at the ratio of H_2/SiH_4 flow-rates of 30→20. (c) External quantum efficiency spectra of solar cell with $\mu\text{-Si:H}$ i-layer deposited at the ratios of H_2/SiH_4 flow-rates of 18, 30→20



and two-step intrinsic Si deposition process by $R=30\rightarrow 20$. The cell prepared at $R=18$ shows a typical spectral response for a-Si:H cells to absorb in spectral range (350~700 nm) [14]. However, the $\mu\text{-Si:H}$ single cell without amorphous incubation layer responded from red to infrared light (700~900 nm). Thus, it was confirmed that the $\mu\text{-Si:H}$ solar cell fabricated by HWP-PECVD at a high pressure of 100 Torr operated well in the long wavelength range. On the other hand, the cell performance was inferior to that of cells fabricated by low pressure PECVD processes. The conversion

efficiency was 1.3 %, and specially short-circuit current (J_{sc}) was 7.3 mA/cm^2 which is very lower than that of previous reports [3, 12, 15]. One prerequisite for high-efficiency $\mu\text{-Si:H}$ solar cell is a low contamination level of impurities in the intrinsic Si absorber layer. Oxygen and nitrogen impurities in $\mu\text{-Si:H}$ behave like donor states, especially the incorporation of oxygen causes an increase in dark conductivity, charge carrier density and spin density. In order to prevent deterioration of cell performance, the critical oxygen and nitrogen impurities level should be below $2 \times 10^{19} \text{ atom/cm}^3$ and $8 \times 10^{18} \text{ atom/cm}^3$ [18]. Figure 6 shows the oxygen and nitrogen SIMS depth profile of $\mu\text{-Si:H}$ single cell without amorphous incubation layer. The measured oxygen and nitrogen concentrations in the HWP-PECVD $\mu\text{-Si:H}$ layer was about 2×10^{20} and $3 \times 10^{19} \text{ atom/cm}^3$, respectively that was increased by one order of magnitude compared with critical impurity level. We guess that the impurities could be originated from the deposition chamber and/or ZnO layer, which is comprised of complex mechanism for moving the stage and the device structure.

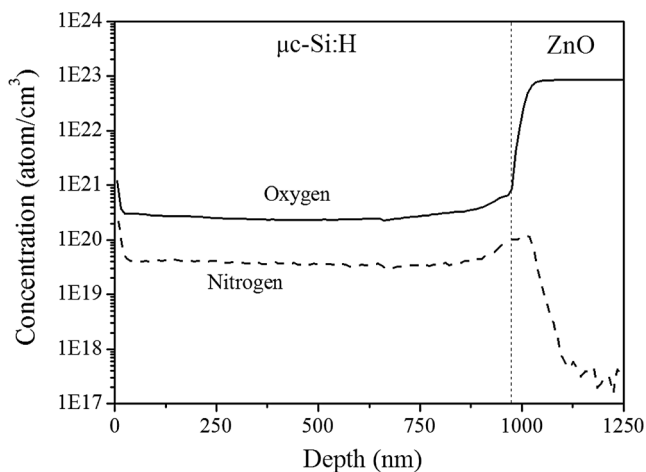


Fig. 6 Oxygen and nitrogen SIMS depth profiles of solar cell with $\mu\text{-Si:H}$ i-layer deposited by HWP-PECVD at the ratio of H_2/SiH_4 flow-rates of 30→20

4 Conclusions

The intrinsic $\mu\text{-Si:H}$ films for photovoltaic layers of thin film solar cells successfully deposited by using the high working pressure plasma-enhanced chemical vapor deposition (HWP-PECVD) technique. The crystalline volume fraction of Si could be controlled by changing the ratio of H_2/SiH_4 flow-

rate. When the $\mu\text{-Si:H}$ n-i-p single junction solar cell was fabricated at the ratio of 18, the intrinsic $\mu\text{-Si:H}$ films contained the 200 nm thick amorphous Si incubation layer, that resulted in the V_{oc} (0.8 V) of a-Si:H single cell performance. On the other hand, when the two-step intrinsic Si deposition process by $R=30\rightarrow 20$ was carried out, homogeneous $\mu\text{-Si:H}$ films responding from red to infrared light through the whole film without amorphous incubation layer could be obtained.

Acknowledgments The present research was supported by the research fund of the Korea Institute of Materials Science, and by the Global Frontier R&D Program (2013-073298) on Center for Hybrid Interface Materials (HIM) funded by the Ministry of Science, ICT & Future Planning.

References

1. H. Keppner, J. Meier, P. Torres, D. Fischer, A. Shah, Microcrystalline silicon and micromorph tandem solar cells. *Appl. Phys. A* **69**, 169–177 (1999)
2. A. Poruba, A. Fejfar, Z. Remeš, J. Špringer, M. Vaněček, J. Kočka, J. Meier, P. Torres, A. Shah, Optical absorption and light scattering in microcrystalline silicon thin films and solar cells. *J. Appl. Phys.* **88**(1), 148–160 (2001)
3. Y. Sobajima, M. Nishino, T. Fukumori, M. Kurihara, T. Giguchi, S. Nakano, T. Toyama, H. Okamoto, Solar cell of 6.3 % efficiency employing high deposition rate (8 nm/s) microcrystalline silicon photovoltaic layer. *Sol. Energy Mater. Sol. Cells* **93**, 980–983 (2009)
4. K. Ouchi, K. Tabuchi, H. Ohmi, H. Kakiuchi, K. Yasutake, Characterization of microcrystalline Si films deposited at low temperatures with high rates by atmospheric-pressure plasma CVD. *Phys. Status Solidi C* **7**(3–4), 545–548 (2010)
5. E. Vallat-Sauvain, U. Kroll, J. Meier, A. Shah, Evolution of the microstructure in microcrystalline silicon prepared by very high frequency glow-discharge using hydrogen dilution. *J. Appl. Phys.* **87**(6), 3137–3142 (2000)
6. P. Alpuim, V. Chu, J.P. Conde, Amorphous and microcrystalline silicon films grown at low temperatures by radio-frequency and hot-wire chemical vapor deposition. *Sol. Energy Mater. Sol. Cells* **78**, 143–180 (2003)
7. Y. Mori, K. Yoshii, H. Kakiuchi, K. Yasutake, Atmospheric pressure plasma chemical vapor deposition system for high-rate deposition of functional materials. *Rev. Sci. Instrum.* **71**(8), 3173–3177 (2000)
8. H. Kakiuchi, M. Matsumoto, Y. Ebata, H. Ohmi, K. Yasutake, K. Yoshii, Y. Mori, Characterization of intrinsic amorphous silicon layers for solar cells prepared at extremely high rates by atmospheric pressure plasma chemical vapor deposition. *J. Non-Cryst. Solids* **351**, 741–747 (2005)
9. J.S. Lannin, *Semiconductors and Semimetals, Part B*, vol. 21 (Academic, New York, 1984)
10. T. Kaneko, M. Wakagi, K.-I. Onisawa, T. Minemura, Change in crystalline morphologies of polycrystalline silicon films prepared by radiofrequency plasma-enhanced chemical vapor deposition using SiF_4+H_2 gas mixture at 350 °C. *Appl. Phys. Lett.* **64**(14), 1865–1867 (1994)
11. P.R. i Cabarrocas, N. Layadi, T. Heitz, B. Drévilion, I. Solomon, Substrate selectivity in the formation of microcrystalline silicon: mechanisms and technological consequences. *Appl. Phys. Lett.* **66**(26), 3609–3611 (1995)
12. C.-H. Lee, M. Shin, M.-H. Lim, J.-Y. Seo, J.-E. Lee, H.-Y. Lee, B.-J. Kim, D. Choi, Material properties of microcrystalline silicon for solar cell application. *Sol. Energy Mater. Sol. Cells* **95**, 207–210 (2011)
13. Y. Tawada, M. Kondo, H. Okamoto, Y. Hamakawa, Hydrogenated amorphous silicon carbide as a window material for high efficiency a-Si solar cells. *Sol. Energy Mater. Sol. Cells* **6**, 299–315 (1982)
14. Y.-J. Lee, M.-S. Choi, D.-H. Kim, C.-S. Kim, M.-K. Song, J.-W. Kang, Y. Jeong, K.-S. Nam, S.-G. Park, S.-H. Kwon, S.Y. Ryu, J.-D. Kwon, Efficient hydrogenated amorphous silicon thin-film solar cells using zinc oxide deposited by atomic layer deposition as a protective interfacial layer. *J. Phys. Chem. C* **116**, 23231–23235 (2012)
15. T. Matsui, M. Tsukiji, H. Saika, T. Toyama, H. Okamoto, Correlation between microstructure and photovoltaic performance of polycrystalline silicon thin film solar cells. *Jpn. J. Appl. Phys.* **41**, 20–27 (2002)
16. R.W. Collins, A.S. Ferlauto, G.M. Ferreira, C. Chen, J. Koh, R.J. Koval, Y. Lee, J.M. Pearce, C.R. Wronski, Evolution of microstructure and phase in amorphous, protocrystalline, and microcrystalline silicon studied by real time spectroscopic ellipsometry. *Sol. Energy Mater. Sol. Cells* **78**, 143–180 (2003)
17. S. Klein, F. Finger, R. Carius, M. Stutzmann, Deposition of microcrystalline silicon prepared by hot-wire chemical vapor deposition: the influence of the deposition parameters on the material properties and solar cell performance. *J. Appl. Phys.* **98**, 024905-1–024905-18 (2005)
18. T. Kilper, W. Beyer, G. Bräuer, T. Bronger, R. Carius, M.N. van den Donker, D. Hrunski, A. Lambertz, T. Merdzhanova, A. Mück, B. Rech, W. Reetz, R. Schmitz, U. Zastrow, A. Gordijn, Oxygen and nitrogen impurities in microcrystalline silicon deposited under optimized conditions: influence on material properties and solar cell performance. *J. Appl. Phys.* **105**, 074509-1–074509-10 (2009)